

The Antimicrobial Effects of Magnolol on the Intracellular pH of *Bacillus subtilis* WB746 and *Escherichia coli* B23

TIM CHIOU, AGUS PO, MICHELLE LIN, TAMMY ROMANUIK, AND ANDREW SHUM

Department of Microbiology and Immunology, UBC

The antimicrobial activity of many cyclic hydrocarbons and phenolic compounds has been ascribed to membrane toxicity. Magnolol, extracted from *Magnolia officinalis*, is a member of a diverse family of plant phenols known to exhibit potent antibacterial effects on Gram-positive, periodontal organisms. However, the mechanism by which this action is realized is hitherto uninvestigated. In this study, we attempted to characterize the molecular basis of the toxic attributes of magnolol by using *Bacillus subtilis* WB746 and *Escherichia coli* B23. Considering the structural features of magnolol and the biological activity of other plant phenols, an effort was made to examine the influence of the compound on membrane energetics, specifically the proton gradient. In order to elucidate this possibility, the antimicrobial efficacy of the compound was first ascertained with the minimum inhibitory concentration (MIC), the affected cells were then studied for morphological aberrations with light microscopy and, finally, the intracellular pH of each cell type was monitored for apparent changes in the Δ pH. Accordingly, we have determined the MIC of magnolol for *B. subtilis* WB746 (25 μ g/ml) and for *E. coli* B23 (50 μ g/ml). Although we could not observe any significant morphological alterations to the cells at these MICs, we did witness a notable drop to the Δ pH of *B. subtilis* WB746. *E. coli* B23, on the other hand, did not appear to experience a similar collapse in proton gradient. As our evidence indicates, it is likely that magnolol exerts its antibacterial effects on the Gram-positive organism by disruption of its energy metabolism at the membrane; however, additional means of action may be responsible, as is probably the case with *E. coli* B23.

Interactions between biological membranes and cyclic hydrocarbons have been found to obstruct bacterial growth and activity (21). In particular, there is a wealth of evidence to impute membrane toxicity to the lipophilic nature of many aromatic compounds; some of these compounds include naphthalene, tetralin and biphenyl (reviewed in 22). Interestingly, the structural characteristics of these organic molecules are collectively displayed in a group of plant phenols called the lignans (2). By definition, lignans are dimers of phenylpropanoid units connected by a β,β -linkage of their side-chain carbons (12). Neolignans, on the other hand, exhibit a slight variation of this theme; unlike the former, these dimers do not associate at the β -position of their side-chain carbons and are restricted in number, as well as phylogenetic distribution (12, 10).

Our present investigation attempts to identify and elucidate the antimicrobial action of a neolignan extracted from *Magnolia officinalis* (8). This phenolic compound, identified as magnolol, has demonstrated a variety of beneficial pharmacological attributes ranging from antiplatelet activity, to free radical scavenging ability and to anti-inflammatory effects (8). Equally important is the repeated indication of its potent antibacterial activity against many periodontal, Gram-positive microbial pathogens (8). Despite the apparent antiseptic properties of magnolol, the mechanism of action of the biphenylic compound is heretofore unexplored, and is therefore a subject of molecular explication. Although the ability to inhibit bacterial growth is not uncommon amongst this family of naturally occurring phenols, the mode of action by other antibacterial lignans such as nor-isoguaiacin and dihydroguaiaretic acid remains inadequately defined (13, 10). In light of the chemical and structural resemblance between magnolol and the other known phenolic compounds, it is possible that magnolol exerts antimicrobial effects by lipophilic induction of membrane toxicity.

Sharing this prized biological feature are the lipophilic phenolics, carvacrol, hydroxycinnamate and allylpyrocatechol (25, 19). Interestingly, the respective structures of all three antimicrobial compounds closely approximate that of the cinnamyl precursor, the monomeric phenylpropanoid unit of all lignans and neolignans (25, 19, 2). In fact, Ultee *et al.* (25) have demonstrated carvacrol's propensity to nestle between lipid acyl chains and cause the expansion of membranes, the leakage of ions and the collapse of proton motive force. Furthermore, a correlation between high antimicrobial activity and the presence of the phenolic hydroxyl group in carvacrol (Fig. 1B) was also established in the same study, accentuating the importance of the hydroxyl moiety to the chemicals'

mechanism of action (25). According to their proposal, this plant phenol may be involved in the transmembrane exchange of periplasmic protons and intracellular cations (25).

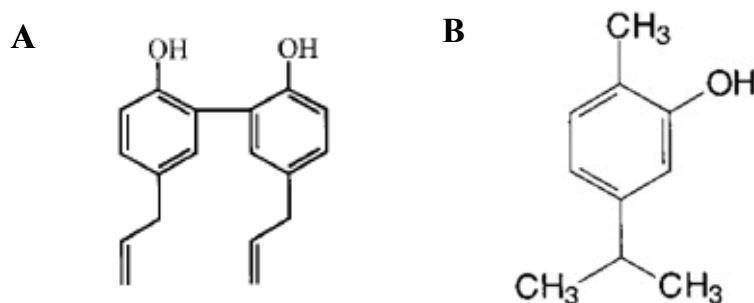


Figure 1. Chemical structures of (A) magnolol and (B) carvacrol

As reviewed in a compendium of studies, lipophilic phenols have been found to partition into the lipid bilayer of cellular membranes, prompting the deleterious disruption of lipid-to-lipid and lipid-to-protein interactions (22, 25). The perturbation of these hydrophobic interactions can elicit such physiological impacts as decreased membrane stability, repressed protein activity (at the membrane) and increased membrane permeability (22). The presence of the propenyl side-chains in magnolol (Fig. 1A) could significantly enhance the overall hydrophobicity of the molecule, and expedite membrane disruption in the affected cells. Meanwhile, the phenolic hydroxyl groups could facilitate the diffusion of periplasmic protons into the intracellular space, dissipating the proton motive force (22). In an attempt to characterize this toxic potential, we hypothesized that magnolol exhibits antimicrobial activity by dissolving the proton gradient that is normally sustained across bacterial membranes for proper physiological functions. To substantiate this supposition, we determined the minimum inhibitory concentration (MIC) of magnolol for *Bacillus subtilis* WB746 (Gram-positive model organism) and *Escherichia coli* B23 (Gram-negative model organism), visualized the treated cells for apparent morphological aberrations with microscopy, and assessed the induction of proton leakage in the respective cells with intracellular pH measurements.

MATERIALS AND METHODS

Bacterial strain and growth conditions. *Bacillus subtilis* WB746 and *Escherichia coli* B23 (both strains obtained from Dr. W. Ramey of the University of British Columbia) were cultivated aerobically at 30°C on Luria-Bertani (LB) agar [0.5% yeast extract (w/v), 1% tryptone (w/v), 0.5% NaCl (w/v) and 1.5% agar (w/v), pH 7.0]. Magnolol (Mag) was supplied by Wako Pure Chemical Industries at 99% purity. The minimum inhibitory concentration (MIC) determination of Mag for both cell types was carried out in LB broth supplemented with the appropriate concentrations of Mag. For MIC determination, cells from both lineages were cultivated aerobically in LB broth at 30°C, shaking 250 rpm, to the appropriate O.D.₅₉₅. Bacteria were prepared for the pH_{in} measurements in a same manner except they were grown at 37°C.

Determination of antibacterial activity. *E. coli* B23 cultures were grown to O.D.₅₉₅ 0.5, and then pelleted via centrifugation (7000 x g for 10 min at 4°C using a Beckman Coulter centrifuge and Beckman JA-17 rotor). The culture was re-suspended in LB broth to a cell density of 0.2 O.D.₅₉₅ before transferring to 96-well microtiter plates. The cells were distributed to the wells, and then diluted to an O.D.₅₉₅ of 0.1 in a total volume of 200 µl. An identical plate was set up for *B. subtilis* WB746. Mag at 0, 25 and 50 µg/ml were added to appropriate wells to determine the MIC. Furthermore, 100 nM nigericin (Nig) and 100 nM valinomycin (Val) (Sigma Aldrich) were added to separate wells as positive controls. Cells were grown at 30°C. O.D.₅₉₅ readings were taken at 0, 40, 70, 105, 140 and 180 min using a Bio-Rad 3550 Microplate Reader. Readings were normalized with a LB blank.

Digital-imaging brightfield microscopy. Cultures left over from the MIC determination final time point were centrifuged (14,000 rpm for 5 minutes using an Eppendorf microcentrifuge) and the cell pellet was resuspended in fresh LB. The *B. subtilis* WB746 and *E. coli* B23 cells treated with 0, 25 and 50 µg/ml of Mag were Gram-stained (11). Cells treated with 100 nM Nig and 100 nM Val were also Gram-stained. The slides were viewed using digital-imaging brightfield microscopy. Nine random fields of each slide were photographed at 470 X magnification with a light microscope (Unilux-12) connected to a Kodak MDS 290 Zoom Digital Camera.

Intracellular pH measurements. The protocol for intracellular pH measurements has been described in previous studies (4, 25). *E. coli* B23 and *B. subtilis* WB746 cells were initially grown to 0.5 O.D.₅₉₅, and then harvested and washed three times with equal volume of 50 mM HEPES-HCl buffer (pH 7.0). For *E. coli* B23, this buffer was supplemented with 5 mM EDTA. The washed cells were incubated with 1.5 µM of carboxyfluorescein diacetate succinimidyl ester (cFDASE, Molecular Probes) for 10 min at 37°C. cFDASE is hydrolysed in the cell to cFSE (carboxyfluorescein succinimidyl ester) and then conjugated to aliphatic amines (25). After being incubated with 10 mM glucose for 30 min at 37°C to eliminate non-conjugated cFSE probe, the cells were washed twice with 50 mM K₂HPO₄ buffer (pH 7.0). For *E. coli* B23, the K₂HPO₄ buffer was supplemented with 10 mM MgCl₂. A third wash with K₂HPO₄ buffer, with no MgCl₂ for either *E. coli* B23 or *B. subtilis* WB746 cells was conducted. The cells were then put on ice and used either for a pH calibration curve or a 12-min time course assay.

A pH calibration curve was constructed with cells suspended in pH buffers consisting of: 50 mM glycine, 50 mM citric acid, 50 mM Na₂HPO₄•2H₂O and 50 mM KCl, adjusted to pH 6.0, 7.0, 8.0, and 9.0 with either NaOH or HCl. The pH buffers in which *E. coli* B23 was suspended required additional supplementation of 5 mM of EDTA to facilitate uptake of the probe. Both 100 nM Nig and 100 nM Val were then added to the cell suspensions to equilibrate the pH_{in} and pH_{out}. Fluorescence intensity units (FIU) were measured at excitation wavelengths of 490 nm (pH-sensitive) and 360 nm (pH-insensitive) using an emission wavelength of 515 nm in a Turner® Quantech™ Digital filter fluorometer (Model No. 109323). The appropriate background readings were subtracted from the raw data.

Twelve-minute time course assays were conducted to measure pH_{in}. Three ml of 50 mM K₂HPO₄ buffer (pH 7.0) was added to a plastic cuvette. The FIUs were measured at one-minute intervals. At the 1- and 3-minute time points, bacterial cell suspension and 10 mM glucose were transferred to the cuvette, respectively. At 7 min, the MIC of Mag was added (50 µg/ml for *E. coli* B23 and 25 µg/ml for *B. subtilis* WB746). In between fluorescence measurements incubation temperature was kept constant at 37°C and the samples were continually stirred. Using the calibration curve above and the polynomial equation of the line, the 490/360 nm ratios were converted into pH_{in} values. Since Mag was excited at 360 nm, a background reading was subtracted from all measurements.

RESULTS

Minimum inhibitory concentration (MIC). In order to assess the antimicrobial activity of Mag, the MICs for *Bacillus subtilis* WB746 and *Escherichia coli* B23 were determined. As expected, the *B. subtilis* WB746 control (0 µg/ml of Mag) exhibited exponential growth (Fig. 2A). In contrast, *B. subtilis* WB746 cultures separately treated with 25 and 50 µg/ml of Mag showed considerable reduction in growth, compared to the control. Accordingly, the MIC of Mag for *B. subtilis* WB746 was confirmed to be 25 µg/ml. In a different study, a similar MIC value for this Gram-positive organism was derived (8). As anticipated, Nig and Val successfully reduced the O.D.₅₉₅ of the culture in a manner comparable to that of Mag.

In contrast, Mag's antimicrobial activity was less effective against *E. coli* B23. The MIC for *E. coli* B23 was ascertained to be 50 µg/ml because cell growth was modulated at that concentration (Fig. 2B). In addition, Nig and Val were not effective against *E. coli* B23. Since the porin channels of *E. coli* B23's outer membrane function to exclude molecules greater than 600-700 Da (15), it is conceivable that Val (1111 Da) and Nig (747 Da) were denied access into the cell.

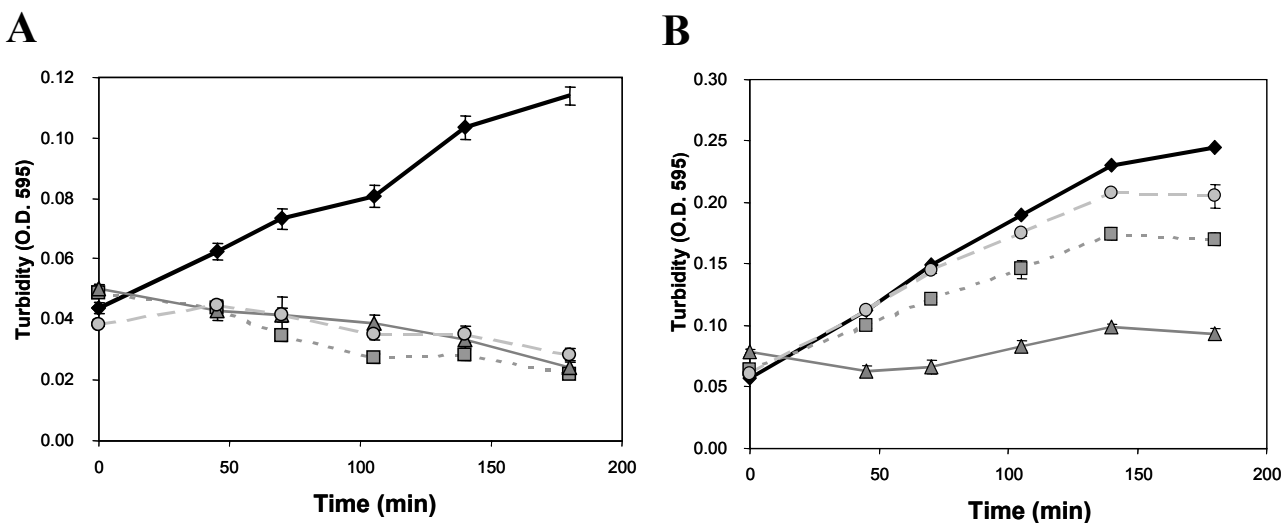


Figure 2. MIC determination of magnolol for *B. subtilis* WB746 (A) and *E. coli* B23 (B). Cells were added to 96-well microtiter plates and monitored at 30°C. Magnolol at 0 µg/ml (◆), 25 µg/ml (■), 50 µg/ml (▲), a mixture of 100 nM of valinomycin and nigericin (●) each were added at 0 min. The turbidity (O.D.₅₉₅) of the wells were taken at regular time-intervals.

Note: under ideal conditions (37°C and good aeration), the doubling time of *E. coli* B23 and *B. subtilis* WB746 should typically be 45 min in nutrient broth (11). In our MIC test, however, the doubling times of *E. coli* B23 and *B. subtilis* WB746 were 70 min and 100 min, respectively. Inadequate aeration of the 96-well microtiter plate could have contributed to this apparent hindrance in cell growth; this effect was especially pronounced in an obligate aerobe such as *B. subtilis* WB746.

Digital-imaging brightfield microscopy. Photographs of Mag-untreated, Mag-treated and Val-Nig-treated cells were obtained and examined for evidence of physical alteration to bacterial morphologies. Comparison between these cells did not offer striking differences in cell shape, cell size, chain length and uptake of Gram-stain (data not shown). Since the target of Mag's antimicrobial action remains largely unknown, light microscopy alone may be inadequate to visualize its effects on the cytoplasmic membranes of *B. subtilis* WB746 and *E. coli* B23.

Intracellular pH measurement. With the intention of elucidating Mag's ability to perturb membrane energetics, the pH_{in} of Mag-treated *B. subtilis* WB746 and the pH_{in} of Mag-untreated *B. subtilis* WB746 were contrasted. In Figure 3, the calibration curve was constructed with the following polynomial equation: $y = -0.9012x^2 + 18.139x - 71.469$. This formula was used to determine the pH_{in} of *B. subtilis* WB746. The emissions at 490 and 360 nm excitation wavelengths (in FIU) were derived for Mag-treated cells (Fig. 4A) and Mag-untreated cells (Fig. 4B). The ratios of these emissions (490/360 nm) were processed, and then presented in Figure 5 to calculate the values for pH_{in} using the aforementioned polynomial equation. Although the original protocol developed by Breeuwer et al. adopted 440 nm as the pH-insensitive wavelength (4), our results indicated that 360 nm was an equally viable candidate (data not shown).

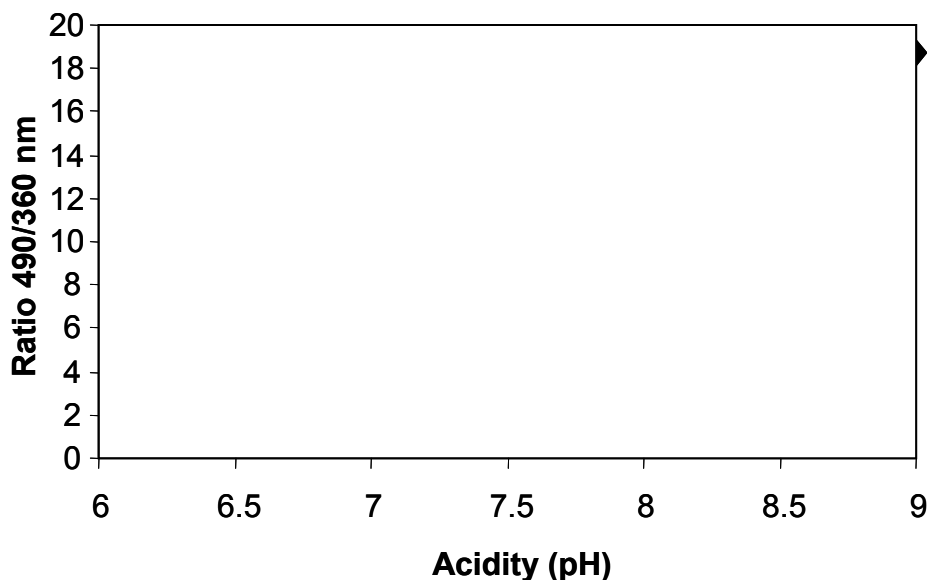


Figure 3. The relationship between the pH and the ratio (490/360 nm) of cFSE in *B. subtilis* WB746. The pH_{in} and pH_{out} were equilibrated with valinomycin (100 nM) and nigericin (100 nM).

In an attempt to monitor the effects of Mag on *B. subtilis* WB746, time-course assays were performed over 12 min. As expected, an apparent increase in the FIU (490 nm) was observed following the addition of cFSE-labelled cells to the phosphate buffer at the 1-min time point (Fig. 4A and B). Glucose, on the other hand, did not appear to contribute to the background signals and the quenching of light emissions. However, when the cell suspension was supplemented with Mag at the 7-min time point, a notable drop in FIU (490 nm) was observed (Fig. 4A). This marked decrease in the pH-sensitive fluorescence was not detected in the Mag-negative sample (Fig. 4B). Evidently, since the FIU at 360 nm is pH-insensitive, the fluorescence intensity of cFSE was not affected by variations in pH (Fig. 4A and B). The ratios of fluorescence at 490/360 nm for Mag-treated and Mag-untreated *B. subtilis* WB746 were determined (Fig 5). The ratio dropped by about 1.6 units immediately after Mag treatment, and then maintained a difference of approximately 1.1 units. Using the calibration curve (Fig. 3), the appropriate fluorescence ratios were converted into pH_{in} values. In Figure 5, the pH_{in} of *B. subtilis* WB746 prior to addition of Mag was 7.4, and it decreased to 7.1 following Mag treatment. This reduction in pH_{in} (by ≈ 0.3 units) did not materialise in the Mag-untreated cells. It should be noted here that the pH of the external milieu (i.e. the phosphate buffer) was approximately 7.0.

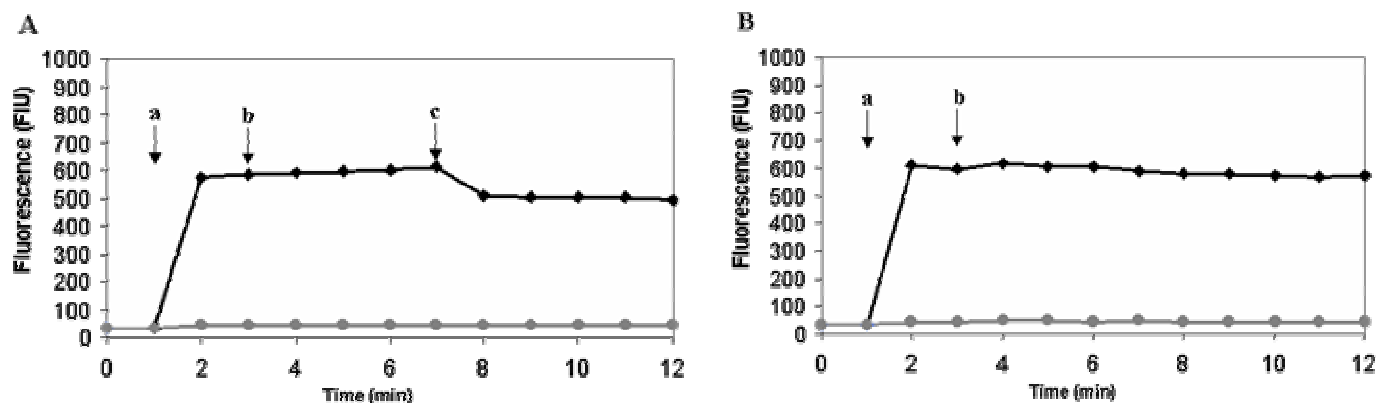


Figure 4. Fluorescence intensity of (A) magnolol-treated and (B) magnolol-untreated *B. subtilis* WB746 at excitations of 490 nm (◆) and 360 nm (●). The emission wavelength was at 515 nm. The following additions were made at the times indicated by the arrows: a, cells suspension; b, glucose (10 mM); c, magnolol (25 μ g/ml).

Previous findings have suggested that the pH_{in} of *B. subtilis* WB746 ranges from 7.5 to 8.0 (3), which is similar to the pH value that we determined before Mag treatment. The observed drop in pH_{in} implies that the pH gradient (ΔpH) normally sustained across the cytoplasmic membrane was collapsed; hence, the pH_{in} approximated the pH_{out} . Had we formulated our phosphate buffer with a higher acidity, this decline in pH_{in} could have been more significant and dramatic than that which was documented in our study (25). Furthermore, in an earlier trial, the addition of Val and Nig to a suspension of *B. subtilis* WB746 previously treated with Mag did not prompt a further decrease in pH_{in} , suggesting that Mag alone has the capacity to equilibrate the pH_{in} and pH_{out} of the affected organisms (data not shown).

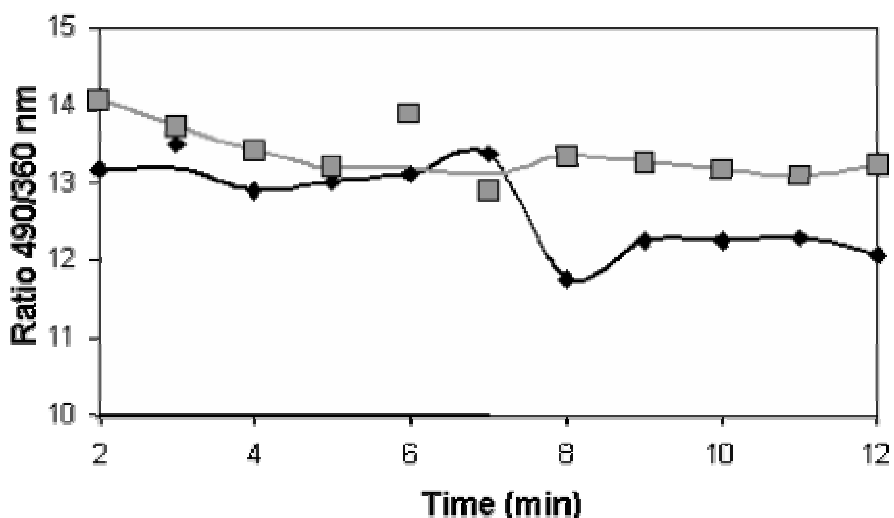


Figure 5. The 490/360 nm ratio of cFSE in magnolol-treated (◆) and -untreated (■) *B. subtilis* WB746 cell suspensions. The emission wavelength was set at 515 nm. The following additions were made at the times indicated by the arrows: a, glucose (10 mM); b, Mag (25 μ g/ml).

Unfortunately, the pH_{in} measurements of Mag-treated and Mag-untreated *E. coli* B23 could not be adequately performed due to insufficient uptake and/or retention of the fluorescent probe. Indeed, we have found that it is difficult to equilibrate the pH_{in} and pH_{out} of *E. coli* B23 with Val and Nig, even with EDTA supplementation. This obstacle is attributable to the fact that *E. coli* membrane exhibits poor permeability to some antibiotics and to cFDASE (20). The passive uptake of a bulky molecule such as cFDASE (557 Da) was probably retarded at the outer membrane of this Gram-negative organism. Moreover, since our *E. coli* B23 culture was grown to late-log phase (a turbidity of about 0.8 O.D.₅₉₅) prior to the addition of the fluorescent label, the cells may have entered a different physiological state that precludes the uptake and/or retention of cFDASE. As toxic metabolites built up in the medium, *E. coli* B23 growing in the late-log phase likely expressed OmpC, a smaller porin, in preponderance over OmpF, a larger porin, to impede the entry of toxic waste products (14). This adaptation could have resulted in a less permeable membrane, obstructing the uptake of the probe (14). Although we could not establish the effects of Mag on the membrane energetics of *E. coli* B23 in the final trial, we did manage to label the cells successfully in the preliminary trial (when the culture was grown to a turbidity of 0.5 O.D.₅₉₅). Results from this preliminary trial were not included in this study due to a separate complication concerning machine calibration. However, in this preliminary attempt, we did not observe a conspicuous reduction in the ratio of 490/360 nm following Mag treatment, denoting the possibility that the inhibition of *E. coli* B23 by Mag may involve different mechanism(s) from the one proposed for *B. subtilis* WB746.

DISCUSSION

In this study, the antimicrobial effect of Mag was shown to be more effective against the *B. subtilis* WB746 than *Escherichia coli* B23. The MIC results show that growth of *B. subtilis* WB746 and *E. coli* B23 were inhibited by 25 $\mu\text{g/ml}$ and 50 $\mu\text{g/mL}$ of Mag respectively. The MIC for *E. coli* B23 is in agreement with a paper previously published by another group (8). The MIC for *B. subtilis* WB746, on the other hand, differs from the results obtained in the same study, which stated that 100 $\mu\text{g/mL}$ of Mag is required for inhibition. This potentially significant difference in MIC between the two studies can be attributed to variations in strains and growth conditions. Additionally, the MIC experiment in this report was performed using liquid culture, whereas the other group utilized a disk diffusion agar assay. Compared to being grown on a solid medium, free cells grown in liquid broth are more susceptible to phenols and the ensuing increase in membrane permeability (7). Cells grown on a solid medium are in much closer proximity to each other. Consequently, intracellular metabolites lost from one cell due to increased membrane permeability may be more readily taken up by surrounding cells (7). Since these cells were able to support each other in a mutualistic manner, a higher concentration of Mag was required.

Results from Figure 4A and 5 demonstrated that the pH_{in} in *B. subtilis* WB746 was equilibrated to the pH_{out} , suggesting that the antimicrobial effect was induced by collapse of pH gradient. The significance and implications of this collapse can be described by the following equation that relates free energy generation to the PMF:

$$\Delta p = \Delta\psi - 59 \Delta\text{pH} \text{ (in mV)}$$

Δp pertains to proton motive force, $\Delta\psi$ refers to electrical potential and ΔpH ($\text{pH}_{\text{in}} - \text{pH}_{\text{out}}$) denotes chemical potential (1). This equation suggests that if $\Delta\psi$ becomes more positive (due to unregulated influx of cations into the cytoplasm from the periplasm) and/or if ΔpH decreases (due to unregulated diffusion of protons from the periplasm into the cytoplasm), Δp would become more positive. Subsequently, the affected cells would experience a drop in PMF; the ability to generate ATP would be compromised (L. Eltis, personal communication). At the moment, it is unclear how Mag affects $\Delta\psi$. A separate experiment is needed to examine how the electrical potential is affected by Mag.

One hypothesis that explains the disruption of PMF in *B. subtilis* WB746 entails phenolic hydroxyl groups on Mag. A study done on carvacrol, another plant-derived phenolic antibiotic, suggests that the mechanism of action involves the association with cation and the subsequent diffusion through the cytoplasmic membrane towards the cytoplasm. The succeeding dissociation of the proton releases the proton into the cytoplasm. Carvacrol then returns to the external environment with a cation. Repetition of this action eventually results in the net diffusion of proton across into the cytoplasm, decreasing the ΔpH , thereby collapsing the pH gradient (25). Due to Mag's structural similarity with carvacrol (Fig. 1B), it is believed that the proton gradient across *B. subtilis* WB746 membrane may have been disrupted through similar mechanisms.

A drop in pH_{in} from 7.4 to 7.1 in *B. subtilis* WB746 indicates that the proton gradient was collapsed by Mag. The structure of Mag may help explain the mechanism behind this dissipation. Mag contains two phenolic hydroxyl groups that can easily be deprotonated due the delocalization of electrons into the benzene ring and the conjugation of double bonds. The ease of deprotonation suggests that the pK_{a} of the phenolic hydroxyl groups are low, meaning that Mag will more readily bring protons in to the cell and accelerate the rate of pH gradient collapse. Accordingly,

with the resulting collapse of the PMF, the organism will be starved of energy needed for most vital cellular functions, making it impossible for the cells to grow.

An alternative hypothesis to explain the collapse of the proton gradient involves the insertion of Mag into the membrane. The partition of Mag into the membrane of *B. subtilis* WB746 could result in disruption of lipid-to-lipid and lipid-to-protein interactions, leading to expansion of the cytoplasmic membrane (22). The destabilized membrane could contribute to the diffusion of ions and intracellular metabolites such as ATP and nucleotides across the cytoplasm into the external ambience, thus diminishing cell viability. Considering that the membrane can be repaired by *B. subtilis* WB746 (26), destabilization of the membrane alone (by a phenolic compound) may be insufficient to inhibit growth. If *B. subtilis* WB746 were able repair the membrane faster than the rate at which the membrane is destabilized by Mag, the viability of the cell could be sustained.

The difference in membrane composition of *B. subtilis* WB746 and *E. coli* B23 may also explain the stronger Mag efficacy against the former. Being Gram-negative, *E. coli* B23 has lipopolysaccharide (LPS) on its outer membrane that makes insertion of a hydrophobic molecule, such as Mag, more challenging and less favoured (22). Furthermore, Gram-negative bacteria in general have a higher tolerance for lipophilic compounds than Gram-positive bacteria. It is known that Gram-negative bacteria are able to accommodate the phenol by converting *cis* fatty acids in their membrane to *trans* fatty acids, thus reducing membrane fluidity (22). This adaptation increases the stability of membrane and making it less susceptible to proton leakage. In addition, Gram-negative bacteria are known to alter LPS, increasing its hydrophilic property, thus conferring transfer resistance to hydrophobic compound (22).

Evidence for the stronger Mag-induced antibacterial activity in *B. subtilis* WB746 may also be found in the electron transport chain (ETC) composition. *E. coli* B23 has many additional ETC enzymes compared to *B. subtilis* WB746. For example, in addition to NADH dehydrogenase, *E. coli* B23 has fumarate reductase and nitrate reductase that allow for anaerobic respiration. *B. subtilis* WB746, on the other hand, has neither enzyme (L. Eltis, personal communication). The implications of this difference are significant in that it is possible that Mag inhibits key enzymes in the ETC. CoQ contains a coupling site that translocates protons from the intracellular matrix to the periplasm, creating a proton gradient. If Mag inhibits NADH dehydrogenase in *B. subtilis* WB746, the proton gradient could not be maintained. In *E. coli* B23, however, the Mag-induced inhibition of NADH dehydrogenase can be compensated with the other coupling proteins, such as the aforementioned fumarate reductase and nitrate reductase, to maintain the proton gradient. For this reason, Mag was less deleterious against *E. coli* B23. This proposed mechanism is further supported by other antibacterial lignans such as nor-isoguaiacin and dihydroguaiaretic acid (NDGA). Both lignans have been shown to inhibit key components in the mitochondrial electron transport systems by inhibiting NADH-oxidase (16). Since little difference exists in the ETC composition between mitochondria and respiring aerobes, the fact that these lignans inhibit ETC proteins argues for the possibility that Mag may indeed inhibit key ETC enzymes.

Data from our MIC experiment imply that Mag inhibits *E. coli* B23 by mechanisms apart from the one proposed, since equilibration of pH_{in} and pH_{out} was not observed. Considering that a lignan derivative called oxolinic acid is found to exert genotoxic effects on prokaryotic cells by inhibiting the ligase activity of prokaryotic type II topoisomerase, gyrase (6, 24, 23), it is possible that Mag inflicts DNA damages by an analogous mode of action. In fact, this inhibition can lead to the formation of protein-associated double-strand DNA breaks.

Although the 490/360 nm ratios in Fig. 5 are intrinsically dependent on the FIU measurements in Fig. 4, the apparent visual disparity between the two figures could be explained by examining anomalous data points. Specific anomalies include the ratio at the 3-min time point for the Mag-untreated cells and the ratio at the 6-min time point for the Mag-treated cells. While these data points did not fit the major trends, they did not significantly impair our conclusions as a sufficient number of data points were collected. These anomalies were most likely caused by errors in the initial FIU measurements. Since the 490 nm measurements were approximately 10 fold larger than the 360 nm measurements, small errors in the latter would translate into an apparently larger error in the 490/360 nm values. Furthermore, the 490/360 nm value at the 8-min time point appears to be undershot in the Mag-treated cells. We speculate that the decline in pH_{in} at this particular time point represents the initial effect of Mag on *B. subtilis* WB746, and that the ensuing increase in pH_{in} signifies an adaptive response to mitigate the deleterious impact of the compound on cells' bioenergetics. It is possible then that the small decrease in pH_{in} at the 12-min time point indicates a gradual corrosion in the cells' ability to accommodate the physiological stress persistently exerted by Mag. However, the time-course assay will have to be prolonged and repeated in order to evince this trend.

Currently, this is the first experiment that investigates the mechanisms of antimicrobial activity of Mag. Since many antibiotics in the market are toxic to humans, understanding the mechanism of Mag action may prove beneficial in creating a new generation of antibiotics. Mag is not cytotoxic to the human cell and may, therefore, be applied to a wide array of pharmaceutical, food and medical settings (5).

In this study we have established a link between reduced cell viability and diminished proton gradient in *B. subtilis* WB746 treated with Mag. This observation indicates the compound's potential to act as a membrane toxin, upsetting the bioenergetics and the pH homeostasis of the Gram-positive cell. However, due to experimental complications, we could not obtain a comparable outcome in *E. coli* B23 treated with Mag. Nevertheless, since a conspicuous decrease in the Δ pH was not witnessed in the results, it is possible that Mag discharges its inhibitory effects on *E. coli* B23, as well as on *B. subtilis* WB746, by alternative and/or additional mechanisms.

FUTURE EXPERIMENTS

Partition coefficient of magnolol in membrane/buffer. To understand the correlation between lipophilicity and membrane toxicity (22), it is important that the partition coefficient ($P_{\text{membrane/buffer}}$) of Mag be determined. In tandem with our analysis of this phenolic compound, this index of hydrophobicity will give a more robust prediction of the effect of Mag on intact cells. The method for determining this coefficient has been described in previous works (22). Liposomes from *Bacillus subtilis* WB746 and *Escherichia coli* B23 can be extracted through sonication, and then suspended in 50 mM HEPES-KOH buffer (pH 7.0). To derive the $P_{\text{membrane/buffer}}$ value of Mag, varying amounts of the neolignan will have to be transferred to the membrane/buffer suspension for an hour of incubation at room temperature. Once the partitioning process is complete, extra-liposomal Mag should be removed from the suspension and the pelleted liposomes dissolved in nonane-containing hexane. The samples should be analyzed by gas chromatography with the specified temperature program. If Mag is indeed as hydrophobic as we postulated, then we would expect more Mag distributed in the liposomal phase than that which is recovered in the aqueous phase.

Leakage of ATP. Since the destabilization of the cytoplasmic membrane and leakage of protons and/or ions can impinge on the cytoplasmic membrane's energy-transducing systems, it is conceivable that an incursion on membrane permeability may instigate the detrimental leakage of ATP. Therefore, ATP leakage should be analyzed. In a previous study (25), the cells of interest were washed and concentrated in a fashion similar to that which is described for intracellular pH measurements (Materials and Methods). The cell suspensions were then supplemented with the appropriate amounts of Mag in a time-course. At regular time-intervals, small volumes of the cell samples were removed for [ATP] measurements. The extracellular and intracellular concentrations of ATP can be determined with a BO1243-107 ATP assay kit. If Mag causes ATP leakage, we should expect the extracellular concentration of ATP to increase considerably following the addition of this neolignan.

ACKNOWLEDGEMENTS

We would like to thank Dr. W. Ramey, K. Smith, E. Hinze, Dr. G. H. N. Towers, Dr. J. Davies and Dr. L. Eltis for their helpful advice, expertise and operational assistance. Lastly, we want to consign our deepest gratitude to all the good people of the media room.

REFERENCES

1. Anraku, Y., and R. B. Gennis. 1987. The aerobic respiratory chain of *Escherichia coli*. Trends Biochem. Sci. **12**:262-266.
2. Ayres, D. C., and J. D. Loike. 1990. Introduction, p. 1-10. In Lignans: chemical, biological and clinical properties. Cambridge UP, New York.
3. Booth, I. R. 1985. Regulation of cytoplasmic pH in bacteria. Microbiol. Rev. **49**:359-378.
4. Breeuwer, P., J. L. Drocourt, F. M. Rombouts, and T. Abee. 1996. A novel method for continuous determination of the intracellular pH in bacteria with the internally conjugated fluorescent probe 5 (and 6-) -carboxyfluorescein succinimidyl ester. Appl. Environ. Microbiol. **62**:178-183.
5. Chang, B., Y. Lee, Y. Ku, K. Bae, and C. Chung. 1998. Antimicrobial activity of magnolol and honokiol against periodontopathic microorganisms. Planta. Med. **64**:367-369.
6. Gellert, M., K. Mizuchi, M. H. O'Dea, T. Itoh, and J. L. Tomizawa. 1977. Nalidixic acid resistance: A second genetic character involved in DNA gyrase activity. Proc. Natl. Acad. Sci. U. S. A. **74**:4772-4776.
7. Heipieper, H. J., K. Heribert, and H. J. Rehm. 1991. Influence of phenols on growth and membrane permeability of free and immobilized *Escherichia coli*. Appl. Environ. Microbiol. **57**:1213-1217.
8. Ho, K.Y., C. C. Tsai, C. P. Chen, J. S. Huang and C. C. Lin. 2001. Antimicrobial activity of honokiol and magnolol isolated from *Magnolia officinalis*. Phytother. Res. **15**:139-141.
9. Huismand, O., and R. d'Ari. 1981. An inducible DNA replication-cell division coupling mechanism in *Escherichia coli*. Nature **290**:797-799.
10. MacRae, W. D. 1984. Biological activities of lignans. Phytochem. **23**:1207-1220.
11. Madigan, M. T., J. M. Martinko, and J. Parker. 1997. Microbial ecology, p. 533-605. In Brock biology of microorganism. Prentice-Hall, New Jersey.
12. Moss, G. P. 2000. Nomenclature of lignans and neolignans. Pure Appl. Chem. **72**:1493-1523.
13. Nakatani, N., K. Ikeda, H. Kikuzaki, M. Kido, and Y. Yamaguchi. 1988. Diaryldimethylbutane lignans from *Myristica argentea* and their antimicrobial action against *Streptococcus mutans*. Phytochem. **27**:3127-3129.

14. **Neidhardt, F. C., J. L. Ingraham, and M. Schaechter.** 1990. Multigene systems and global regulation, p. 351-388. *In* The physiology of the bacterial cell: a molecular approach. Sinauer Associate Inc., Massachusetts.
15. **Neidhardt, F. C., J. L. Ingraham, and M. Schaechter.** 1990. Structure and function of cell parts, p. 30-60. *In* The physiology of the bacterial cell: a molecular approach. Sinauer Associate Inc., Massachusetts.
16. **Pardini, R. S., C. H. Kim, R. Biagini, R. J. Morris, and D. C. Fletcher.** 1973. Inhibition of mitochondrial electron-transport system by nor-isoguaiaicin. *Biochem. Pharma.* **22**:1921-1925.
17. **Quillardet, P., and M. Hofnung.** 1985. The SOS chromotest, a colorimetric bacterial assay for genotoxins procedures. *Muta. Res.* **147**:65-78.
18. **Quillardet, P., O. Huisman, R. d'Ari, and M. Hofnung.** 1982. The SOS chromotest: direct assay of the expression of the gene *sfi A* as a measure of genotoxicity of chemicals. *Biochimie.* **64**:797-801.
19. **Ramji, N., N. Ramji, R. Iyer, and S. Chandrasekaran.** 2002. Phenolic antimicrobials from piper betle in the prevention of halitosis. *J. Ethnopharma.* **83**:149-152.
20. **Riondet, C., R. Cachon, Y. Waché, G. Alcaraz, and C. Divies.** 1997. Measurement of the intracellular pH in *Escherichia coli* with the internally conjugated fluorescent probe 5- (and 6-) carboxyfluorescein succinimidyl ester. *Biotech. Techniq.* **11**:735-738.
21. **Sikkema, J., J. A. M. de Bont, and B. Poolman.** 1993. Interactions of cyclic hydrocarbons with biological membranes. *J. Bio. Chem.* **269**:8022-8028.
22. **Sikkema, J., J. A. M. de Bont, and B. Poolman.** 1995. Mechanism of membrane toxicity of hydrocarbons. *Microbiol. Rev.* **59**:201-222.
23. **Sugino, A., C. L. Peebles, K. N. Kreuzer, and N. R. Cozzarelli.** 1977. Mechanism of action of nalidixic acid: purification of *Escherichia coli nala* gene product and its relationship to DNA gyrase and a novel nicking-closing enzyme. *Proc. Natl. Acad. Sci. U. S. A.* **74**:4767-4771.
24. **Synder, M., and K. Drlica.** 1979. DNA gyrase on the bacterial chromosome: DNA cleavage induced by oxolinic acid. *J. Mol. Biol.* **131**:287-302.
25. **Ultee, A., M. H. J. Bennik, and R. Moezlaar.** 2002. The phenolic hydroxyl group of carvacrol is essential for action against the food-borne pathogen *Bacillus cereus*. *Appl. Environ. Microbiol.* **68**:1561-1568.
26. **Yablonsky, F.** 1982. Alteration of membrane permeability in *Bacillus subtilis* by clofoctol. *J. Gen. Microbiol.* **129**:1089-1095.